Linear sloshing in a 2D rectangular tank with a flexible sidewall

Ida M. Strand[a], Odd M. Faltinsen[a]

[a] *Centre for Autonomous Marine Operations and Systems, Department of Marine Technology, Norwegian University of Science and Technology, Trondheim, Norway*

Abstract

A 2D rectangular sloshing tank with a flexible sidewall have been studied analytically and numerically, with a focus on the coupling between sloshing and the flexible wall. This analysis introduces new knowledge of the effect of internal motions and flow in a membrane structure with a free surface, such as closed flexible fish cages. A framework for analyzing coupled fluid- membrane interaction in the time, and frequency domain in 2D have been developed. The analytical solution gives new knowledge about the effect of the deformations on the linear pressure inside the tank. Coupled eigenfrequencies and the transfer functions for two different membrane lengths due to sway excitation have been found both analytically and numerically. The analytical and numerical results agree. The eigenfrequencies of the system are highly dependent on both the tension and the 2D membrane length. If we consider a given value of tension, then the eigenfrequency of the coupled system is smaller than the sloshing frequency of the rigid tank for any given n. If the tension is small, and we consider a given sloshing frequency of the rigid tank, then there can be more than n eigenfrequencies of the coupled system that is lower than the sloshing frequency of the rigid tank. For large tensions, the eigenfrequencies of the system become the sloshing frequency of a rigid tank. For low tensions, numerical challenges for the direct numerical solution for frequencies close to the natural sloshing frequencies were pointed out.

Keywords: Sloshing, hydroelastic, flexible, aquaculture

1. Introduction

Norway has become the world's largest producer of Atlantic salmon through the use of open net structures in the sea. The aquaculture facilities have grown in both size and number. Currently, the industry faces increased attention on environmental challenges related to fish escapes, sea lice, diseases, and pollution. A possible solution is to use a Closed Flexible Fish Cage (CFFC) with impermeable membrane material instead of nets used in conventional aquaculture net cages. Compared to a net-based structure the behavior of the new membrane-based system changes completely. Multiple model experiments for both still water, (Strand et al., 2014), current, (Lader et al., 2015; Strand et al., 2016) and waves (Lader et al., 2016) have been performed, for various filling levels and geometries.Resonant water motion (sloshing) was observed in model tests with a CFFC both by Rudi and Solaas (1993) and by Lader et al. (2016). All the results showed that the CFFC is flexible, behaves hydro-elastically and that the response is highly dependent on both geometry and filling level.

The deformations and forces on the CFFC depend on both the external and internal hydrodynamic pressure and the structure dynamics. It is crucial to understand the dependency between forces and deformations, to develop models, which predict the correct environmental forces and response. The pressure from the liquid motions (sloshing) inside the bag must be found to solve the general problem. If we can assume that the boundary layer close to the membrane is thin, there are no breaking waves, and there are no interior structures causing flow separation, the flow inside the bag can be assumed potential. The CFFC can have any shape. However, the shapes viewed as most practical are ellipsoidal

Email address: ida.strand@ntnu.no (Ida M. Strand)

and spherical. Sloshing in these shapes are not possible to analyze by analytical methods. To develop theory and understanding of the coupled system, and the coupling between structural response and internal water motions, the system is further simplified to a 2D rectangular sloshing tank with a fabric membrane sidewall. Most considered hydroelastic problems are too complex to analyze analytically, numerical and/ or experimental methods are therefore used. For this particular system, there exists an analytical solution, which can give an understanding of the coupled system and can be utilized for verification of a numerical code, intended used for the end problem.

Liquid sloshing in tanks represents a challenge both in the naval, air and space, civil and in the nuclear industry, and have therefore been thoroughly studied (Faltinsen, 2009; Ibrahim, 2005). In some of these cases, hydroelasticity have an effect. Common for most of these cases is that the structural stiffness of the problem is due to bending stiffness and that the structural natural frequencies are higher than the sloshing frequencies. A comprehensive review is found in Ibrahim (2005).

In the considered system one of the walls is modeled as a fabric membrane, meaning that the tension stiffness dominates, with bending stiffness as a minor effect. When tension dominates, the structural natural frequencies may very well be in the range of the sloshing frequencies. The hydroelastic behavior of a rectangular tank with a fabric membrane sidewall of different lengths has earlier partly been studied by Schulkes (1990). Schulkes (1990) investigated the case where the lower part of one of the side walls was modeled as a membrane. He showed by analytical means that when part of the rigid wall was replaced with a membrane, the eigenfrequencies of the total system decreased. The extent of this decrease in eigenfrequency depend on the proportion of the membrane length relative to the length of the tank wall, and the tension applied to the membrane.

A special case of what we consider is a container with a rigid moving wall, attached to an outside spring. Lu et al. (1997) and Chai et al. (1996) have analytically solved this coupled fluid-structure system and found the pressure contribution on the rigid movable wall. Lu et al. (1997) used a similar method as our analytical method, while Chai et al. (1996) solved the problem by incorporating a wave maker solution.

The hydroelastic analysis of a rectangular tank with a fabric membrane sidewall of different lengths can introduce new knowledge of the effect of internal motions and flow in a membrane structure with a free surface. An analytical solution for the coupled fluid- membrane interaction problem in the time, and frequency domain in 2D have been found. Coupled eigenfrequencies and the transfer functions of wave elevation for two different membrane lengths from sway excitation have been found both analytically and numerically. The effect of hydrostatic pressure is not considered since the end application of the theory and knowledge is with water on both sides of the membrane.

2. Linear sloshing in a 2D rectangular tank with an elastic wall

Our analytical hydrodynamic method can be classified as a multimodal method (Faltinsen, 2009), which has been successful in solving linear and nonlinear sloshing problems within potential flow theory of an incompressible liquid. The method transfers the solution of the Laplace equation for the velocity potential with initial and boundary conditions to a system of ordinary differential equations that, for instance, facilitates analytical hydrodynamic stability analysis, and detection of , multiple solutions and wave regimes. Furthermore, the method facilitates coupling with structural dynamics because acceleration dependent internal load effects can be explicitly identified, both for linear and non-linear sloshing problems.

A two-dimensional rectangular tank with breadth l and mean liquid depth h with a flexible left wall, where the tank is forced with prescribed horizontal tank motion is considered. We define a Cartesian coordinate system Oyz with the origin in the center and at the mean free surface with positive z upwards (see figure 1).

A stretched 2D membrane is assumed, and bending stiffness and structural nonlinearities are neglected. The membrane deformations are represented in terms of structural eigenmodes with unknown time-dependent generalized coordinates $\nu_m(t)$ associated with each dry structural eigenmode $U_m(z)$. A vertical 2D membrane of length L at $y = -l/2$ is fixed at the tank bottom, free surface piercing and

fixed at the upper end, models the flexible wall. In 2D, a flexible membrane is a cable, and the cable theory by Irvine (1981) can be used. The differential equation for the considered membrane is

$$\rho_c d\frac{\partial^2 v(z,t)}{\partial t^2} - T\frac{\partial^2 v(z,t)}{\partial z^2} = F(z,t) \tag{1}$$

Here $\rho_c$and d are the density and thickness of the membrane, respectively. t is the time variable, v is the deformation in the $y-$ direction, T the tension and F is the force component per unit length in the $y-$ direction. The force per unit length on the right hand side of eq. 1 is

$$F(z,t) = \begin{cases} -p, & -h \le z \le 0 \\ 0, & 0 \le z \le L-h \end{cases} \tag{2}$$

where p is the dynamic water pressure.

We will represent the deformation in terms of dry eigenmodes. That means we consider non-trivial solutions of eq. 1 without the effect of the water pressure:

$$\rho_c d\frac{\partial^2 v(z,t)}{\partial t^2} - T\frac{\partial^2 v(z,t)}{\partial z^2} = 0, \tag{3}$$

with harmonic oscillations together with fixed end conditions. The dry eigenmodes of the 2D membrane, are

$$U_m(z) = \sin(\frac{m\pi}{L}(z+h)), \tag{4}$$

which are connected to the dry natural frequency $\lambda_m = \frac{m\pi}{L}\sqrt{\frac{T}{\rho_c d}}$, with L as the length of the 2D membrane. Then the deformation can be expressed as

$$v(z,t) = \sum_m \nu_m(t) U_m(z), \tag{5}$$

where $\nu_m(t)$ are the generalized structure mode amplitudes.

We assume linear potential flow of an incompressible liquid. The velocity potential and the free surface elevation are denoted as Φ and ζ, respectively. The boundary value problem of the linear sloshing problem in a rectangular tank with a flexible wall can be expressed as:

$$\nabla^2\Phi = \frac{\partial \Phi^2}{\partial y^2} + \frac{\partial \Phi^2}{\partial z^2} = 0 \text{ for } -\frac{1}{2}l < y < \frac{1}{2}l, -h < z < 0, \tag{6}$$

$$\left.\frac{\partial \Phi}{\partial z}\right|_{z=-h} = 0,$$

$$\left.\frac{\partial \Phi}{\partial y}\right|_{y=-\frac{1}{2}l} = \dot{\eta}_2 + \sum_m \dot{\nu}_{dm} U_m(z),$$

$$\left.\frac{\partial \Phi}{\partial y}\right|_{y=\frac{1}{2}l} = \dot{\eta}_2,$$

$$\left.\frac{\partial \Phi}{\partial z}\right|_{z=0} = \frac{\partial \zeta}{\partial t}, \tag{7}$$

$$\left.\frac{\partial \Phi}{\partial t} + g\zeta\right|_{z=0} = 0. \tag{8}$$

A dot above the variable means time derivative, $\dot{\eta}_2$ is the prescribed horizontal rigid body tank velocity (sway velocity) and g is the gravitational acceleration. The deformation velocity of the wall is expressed as $\sum_m \dot{\nu}_{dm} U_m(z)$. The boundary value problem for the liquid flow in the tank is illustrated in figure 1.

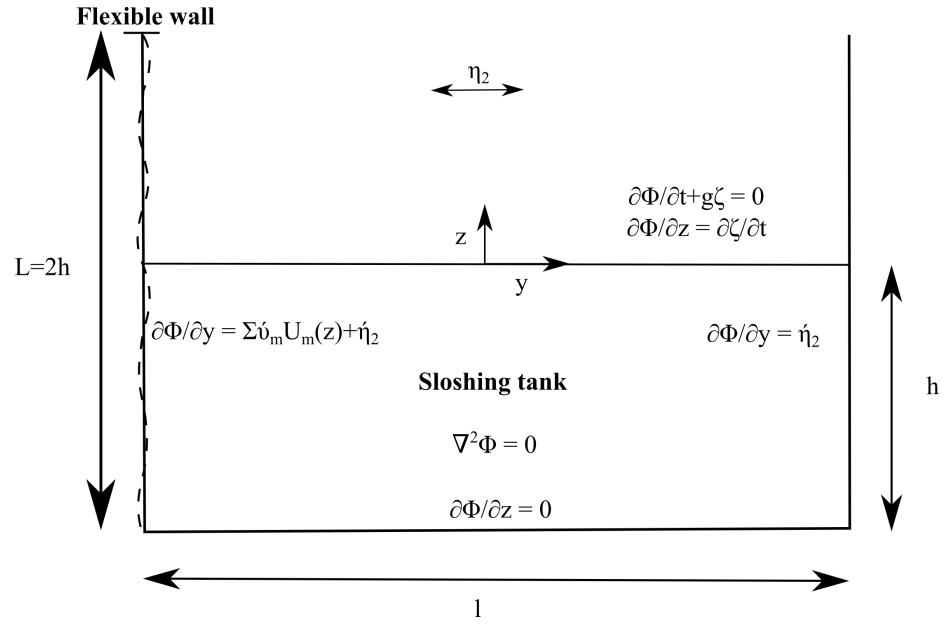

Figure 1: Boundary conditions for a two-dimensional rectangular tank with breadth l and mean liquid depth h with a flexible left wall of length L that is forced with prescribed horizontal tank motions η_2 in the time domain.

2.1. Analytical time-domain solution

The liquid flow can be described analytically by the multimodal method (Faltinsen, 2009). It implies that the free surface elevation ζ is expressed as the Fourier series:

$$\zeta(y,t) = \frac{1}{l}\sum_{m=1} \nu_m(t) \int_{-h}^{0} U_m(z)dz + \sum_{n=1}^{\infty} \beta_n(t) f_n(y) \tag{9}$$

where $f_n(y) = \cos(\pi n(y + \frac{1}{2}l)/l)$, and β_n are the generalized free surface coordinates. The spatially constant term in the Fourier series is a consequence of liquid mass conservation and elastic wall deformations.

The velocity potential Φ is expressed as:

$$\Phi(y,z,t) = \dot{\eta}_2(t)y + \phi(y,z,t) + \sum_{m=1}^{\infty} \Omega_{dm}(y,z)\dot{\nu}_m(t) + C(t) \tag{10}$$

similarly as in Faltinsen (2009), except for their missing spatially constant $C(t)$, which gives an important contribution to the dynamic pressure. The first term in the velocity potential takes care of the body boundary condition associated with the rigid body motions. The terms associated with the deformation potential Ω_{dm} take care of the body boundary conditions due to the membrane deformations. The ϕ term is a sum of sloshing eigenmodes satisfying homogeneous Neumann body boundary conditions, i.e:

$$\phi(y,z,t) = \sum_{n=1}^{\infty} R_n(t)\cos(\pi n(y + \frac{1}{2}l)/l)\frac{\cosh(\pi n(z+h)/l)}{\cosh(\pi n h/l)} \tag{11}$$

where $R_n(t)$ are generalized coordinates for the velocity potential.

The deformation potentials satisfy in addition to the Laplace condition and zero Neumann conditions on $z = -h$ and $y = 0.5l$, the boundary conditions:

$$\left.\frac{\partial \Omega_{dm}}{\partial y}\right|_{y=-\frac{l}{2}} = U_m(z), \qquad -h < z < 0, \tag{12}$$
$$\left.\frac{\partial \Omega_{dm}}{\partial z}\right|_{z=0} = \frac{1}{l}\int_{-h}^{0} U_m(z)dz, \qquad -\frac{l}{2} < y < \frac{l}{2},$$

The latter condition is consistent with conservation of liquid mass and the first term of the Fourier series representation of the free surface given by eq. 9.

To get an analytical solution of $\Omega_{dm}(y,z)$, we represent the wall velocity profile given by $U_m(z)$ as a Fourier series:

$$U_m(z) = \alpha_{0m} + \sum_{k=1}^{\infty} \alpha_{km} \cos(k\pi(z+h)/h), \tag{13}$$

where the Fourier coefficients α_{0m} and α_{km} are found by:

$$\alpha_{0m} = \frac{1}{h}\int_{-h}^{0} U_m(z)dz = 2\frac{L}{hm\pi}\sin^2(\frac{m\pi h}{2L}),$$
$$\alpha_{km} = \frac{2}{h}\int_{-h}^{0} U_m(z)\cos(k\pi(z+h)/h)dz = \frac{2L}{\pi}\frac{kL\sin(\pi k)sin(\frac{m\pi h}{L}) + hm(-1)^k cos(\frac{m\pi h}{L}) - hm}{L^2k^2 - h^2m^2}.$$

Faltinsen (2009, p. 224-225) have presented the following analytical solution

$$\Omega_{dm}(y,z) = -\frac{\alpha_{0m}}{2l}((y-0.5l)^2 - (z+h)^2) - \sum_{k=1}^{\infty}\frac{\alpha_{km}h}{k\pi}\cos(k\pi(z+h)/h)\frac{\cosh(k\pi(y-0.5l)/h)}{\sinh(\pi kl/h)} \tag{14}$$

We must in the end ensure that the total velocity potential satisfies the dynamic and kinematic free surface conditions as given by eq. 7-8. This set up a relation between the generalized coordinates $\beta_n(t)$ and $R_n(t)$, determines $C(t)$ and derives ordinary differential equations for the generalized coordinates β_n. To find a relation between the generalized coordinates $\beta_n(t)$ and $R_n(t)$, the kinematic boundary condition is multiplied with $\cos(\pi n(x+0.5l)/l)$ for $n \geq 1$ and integrated from $-l/2$ to $l/2$. It follows that

$$\dot{\beta}_n(t) = \kappa_n R_n(t) \tag{15}$$

where κ_n is

$$\kappa_n = \frac{\omega_n^2}{g} = \frac{\pi n}{l}\tanh(\frac{n\pi}{l}h) \tag{16}$$

with ω_n as the natural sloshing frequencies for the rigid tank.

To find $\dot{C(t)}$ we integrate the dynamic free surface condition (eq. 8) over the free surface. The result is:

$$\dot{C(t)} = -\sum_{m=1}^{\infty}\overline{\Omega_{dm}}\ddot{\nu}_m(t) - \frac{g}{l}\sum_{m=1}\nu_m(t)\int_{-h}^{0}U_m(z)dz \tag{17}$$

where

$$\overline{\Omega_{dm}} = \frac{1}{l}\int_{-\frac{l}{2}}^{\frac{l}{2}}\Omega_{dm}(y,0)dy = -\frac{\alpha_{0m}}{2l}(\frac{l^2}{3} - h^2) - \sum_{k=1}^{\infty}\frac{\alpha_{km}h^2}{lk^2\pi^2}(-1^k).$$

The ordinary differential equations for $\beta_n(t)$ follows by multiplying eq. 8 with $\cos(\pi n(x+0.5l)/l)$ for $n \geq 1$ and integrating from $-l/2$ to $l/2$. The result is

$$\ddot{\beta}_n + \omega_n^2\beta = -\frac{\gamma_{2n}}{\mu_n}\ddot{\eta}_2 - \sum_m\frac{\gamma_{dnm}}{\mu_n}\ddot{\nu}_m(t) \text{ for } n = 1, 2.., \tag{18}$$

where

$$\mu_n = \frac{\rho l}{2\kappa_n}, \quad \frac{\gamma_{2n}}{\rho_w} = \left(\frac{l}{n\pi}\right)^2 [(-1)^n - 1], \tag{19}$$

$$\frac{\gamma_{dnm}}{\rho} = -\alpha_{0m}\frac{l^2}{\pi^2 n^2} - \frac{1}{\pi^2}\sum_{k=1}^{\infty}\frac{\alpha_{km}(-1)^k l^2 h^2}{l^2k^2 + h^2n^2}. \tag{20}$$

Here γ_{dnm} and γ_{2n} are the hydrodynamic coefficients assosiated with the wall deformations and sway motion, respectively.

Based on the found Φ, the linear dynamic pressure p on the 2D membrane is :

$$\begin{aligned} p &= -\rho_w \frac{\partial \Phi}{\partial t}(-\frac{l}{2}, z) \\ &= -\rho_w \left(\sum_{m=1}^{\infty} (\Omega_{dm}(-\frac{l}{2}, z) - \overline{\Omega_{dm}})\ddot{\nu}_m(t) - \frac{l}{2}\ddot{\eta}_2(t) + \sum_{n=1}^{\infty}\frac{\ddot{\beta}_n(t)}{\kappa_n}\phi_n(-\frac{l}{2}, z) - \frac{g}{l}\sum_{m=1}^{\infty}\int_{-h}^{0} U_m(z)dz\nu_m(t)\right) \end{aligned} \tag{21}$$

where ρ_w is the liquid density. The last part of the pressure contribution comes from $C(t)$ and is a quasi-steady hydrostatic pressure change due to the change in mean free surface position. This pressure part is added in Malenica et al. (2015), but should not as long as one solves a boundary value problem with the same free-surface condition as stated in eq. 7 and eq. 8. An additional confirmation is that we show later, by a numerical solution using the same free surface conditions and the dynamic pressure given as $-\rho_w \partial\Phi/\partial t$, that we get the same results as with the analytical solution.

Ordinary differential equations for the structural mode amplitudes ν_m can now be found by multiplying eq. 1 with the mode $U_j(z)$ and integrating from $z = -h$ to $z = L - h$. This gives

$$\ddot{\nu}_j(t) + \lambda_m^2 \nu_j(t) = \frac{\rho_w}{\mu}\int_{-h}^{0}\frac{\partial\Phi}{\partial t}(-\frac{l}{2}, z)U_j(z)dz, \tag{22}$$

where the generalized modal mass, is $\mu = \rho_c dL/2$. The term on the right hand side of eq. 22 can be rewritten in terms of generalized added mass and restoring coefficients by the following definitions:

$$\int_{-h}^{0}\sum_{m=1}^{\infty}(\Omega_{dm}(-\frac{l}{2}, z) - \overline{\Omega_{dm}})U_j(z)dz\ddot{\nu}_m(t) = -\sum_{m=1}^{\infty}\frac{a_{mj}^{(\Omega)}}{\rho_w}\ddot{\nu}_m(t) \tag{23}$$

$$\int_{-h}^{0}\sum_{n=1}^{\infty}\ddot{\beta}_n(t)\frac{\cosh(\pi n(z+h)/l)}{\kappa_n \cosh(\pi n h/l)}U_j(z)dz = -\sum_{n=1}^{\infty}\frac{a_{nj}^{(\phi)}}{\rho_w}\ddot{\beta}_n(t) \tag{24}$$

$$\frac{g}{l}\sum_{m=1}^{\infty}\int_{-h}^{0}U_m(z)dz\int_{-h}^{0}U_j(z)dz\nu_m(t) = \sum_{m=1}\frac{c_{mj}}{\rho_w}\nu_m(t) \tag{25}$$

$$\frac{l}{2}\int_{-h}^{0}U_j(z)dz\ddot{\eta}_2(t) = \frac{\gamma_{2j}}{\rho_w}\ddot{\eta}_2(t) \tag{26}$$

Superscripts are used on the coupled added mass coefficients $a_{mj}^{(\Omega)}$ and $a_{nj}^{(\phi)}$ to indicate that they are associated with Ω and ϕ, respectively. The consequences are that $a_{mj}^{(\Omega)}$ is frequency independent while $a_{nj}^{(\phi)}$ is frequency dependent. $a_{mj}^{(\Omega)}$ provide coupling between the structural modes, while $a_{nj}^{(\phi)}$ provide coupling between the structural and sloshing modes. The restoring coefficients c_{mj} are associated with quasi- static hydrostatic pressure change due to mean free-surface change described by the first term in the Fourier series (eq. 9) for the free surface elevation. The coefficients γ_{2j} are proportional to coupled generalized added mass between sway and structural modes. The calculation of and expression for the different parts of the pressure contribution is given in the appendix (eq. A.1- eq. A.4).

The total equation for the 2D membrane becomes:

$$\ddot{\nu}_j(t) + \sum_m \frac{1}{\mu} a_{mj}^{(\Omega)} \ddot{\nu}_m(t) + \lambda_m^2 \nu_j(t) + \sum_m \frac{c_{mj}}{\mu} \nu_m(t) = -\sum_n \frac{a_{nj}^{(\phi)}}{\mu} \ddot{\beta}_n(t) - \ddot{\eta}_2(t) \frac{\gamma_{2j}}{\mu}. \tag{27}$$

From eq. 27 it can be seen that the response of a given mode j is dependent on all the other modes, both structural modes, and free surface modes.

It follows from Greens second identity, boundary conditions on mean free surface S_F and mean wetted surface S_B and n as the normal direction to these surfaces that

$$\begin{aligned}
&\int_{S_F+S_B} \left[(\Omega_{dm}(-l/2,z) - \overline{\Omega_{dm}}) \frac{\partial \Omega_{dj}(-l/2,z)}{\partial n} - (\Omega_{dj}(-l/2,z) - \overline{\Omega_{dj}}) \frac{\partial \Omega_{dm}(-l/2,z)}{\partial n} \right] dS \\
&= \int_{-h}^{0} \left[(\Omega_{dm}(-l/2,z) - \overline{\Omega_{dm}}) U_j(z) - (\Omega_{dj}(-l/2,z) - \overline{\Omega_{dj}}) U_m(z) \right] dz = a_{mj}^{(\Omega)} - a_{jm}^{(\Omega)} = 0.
\end{aligned}$$

That means find that $a_{mj}^{(\Omega_d)} = a_{jm}^{(\Omega_d)}$. By exchanging the mode U_j with the Fourier representation in eq. 24, we find that $a_{nj}^{\phi} = \gamma_{dnj}$.

2.2. Analytical frequency-domain solution

We solve both the tank and the 2D membrane problem in the frequency domain, by substituting $\nu_m = \overline{\nu}_m \exp(i\omega t)$ and $\beta_n = \overline{\beta}_n \exp(i\omega t)$ with ω as the forcing frequency in eq. 18 and eq. 27. The result is

$$(\omega_n^2 - \omega^2)\overline{\beta}_n - \omega^2 \sum_m \frac{\gamma_{dnm}}{\mu_n} \overline{\nu}_m = \frac{\gamma_{2n}}{\mu_n} \omega^2 \overline{\eta}_2 \tag{28}$$

$$-\omega^2 \sum_n \frac{a_{nj}^{\phi}}{\mu} \overline{\beta}_n + (\lambda_m^2 - \omega^2)\overline{\nu}_j + \sum_m \frac{1}{\mu}(c_{jm} - \omega^2 a_{mj}^{(\Omega)})\overline{\nu}_m = \omega^2 \frac{\gamma_{2j}}{\mu} \overline{\eta}_2 \tag{29}$$

2.2.1. Estimating the eigenfrequencies of the system

If we combine 28 and 29 we get:

$$-\sum_n \sum_m \frac{\omega^4 a_{nj}^{\phi} \gamma_{dnm}}{\mu \mu_n (\omega_n^2 - \omega^2)} \overline{\nu}_m + (\lambda_m^2 - \omega^2)\overline{\nu}_j + \sum_m \frac{c_{jm} - \omega^2 a_{mj}^{(\Omega)}}{\mu} \overline{\nu}_m = \frac{\omega^2}{\mu}(\gamma_{2j} - \sum_n \frac{\omega^2 a_{nj}^{\phi} \gamma_{2n}}{\mu_n(\omega_n^2 - \omega^2)})\overline{\eta}_2. \tag{30}$$

The natural frequencies of the system is found by looking at the nontrivial solution of eq. 30 for zero excitation ($\eta_2 = 0$). For a given mode j we can see that there are coupling to other modes both in the structural modes (m) and for the sloshing (modes n). The coupling causes the natural frequencies ω_n^* to differ from the natural frequencies ω_n of the rigid tank. Equation 30 will have two limits when it comes to tension T. When tension $T \to \infty$, the dry structural natural frequencies $\lambda_m \to \infty$, and 30 reduces to $\omega_n^* = \omega_n$. Meaning that the eigenfrequencies of the system become the eigenfrequencies of the sloshing problem. On the other hand when $T = 0$, the system still have stiffness from the free surface stiffness term c_{mm}, meaning that $\omega_n^* > 0$ also for the case of zero tension. However, this is a case where the linear 2D membrane theory as described here is not valid, as bending is neglected and will have an influence in reality.

A first estimate of the coupled eigenfrequency of the tank with the elastic wall is that we neglect the coupling effect between structural modes, and only considers one structural mode, together with one free surface mode. We introduce the following wet 2D membrane eigenfrequency as $\lambda_m^* = \sqrt{\frac{\mu\lambda_m^2 + c_{mm}}{\mu + a_{mm}^{(\Omega)}}}$. Here a_{mj}^{Ω} is used to estimate the added mass effect. This gives:

$$\left(-\omega^4 \frac{a_{nm}^{(\phi)} \gamma_{dnm}}{\mu_n(\mu + a_{mm}^{(\Omega)})} + (\omega_n^2 - \omega^2)({\lambda_m^*}^2 - \omega^2) \right) \overline{\nu}_m = 0. \tag{31}$$

Equation 31 is a fourth order directly solvable equation with two possible positive solutions for every parameter combination. An estimate of the first two possible eigenfrequencies, based on the first structural mode ($j = 1$) and the first free surface mode ($n = 1$) are found by:

$$\omega_{1s}^{est}, \omega_{2s}^{est} = \sqrt{\frac{\sigma_1^2 + \lambda_1^{*2} \mp \sqrt{(\sigma_1^2 + \lambda_1^{*2})^2 - 4(1 - \frac{a_{11}^{(\phi)}}{\mu + a_{11}^{(\Omega)}} \frac{\gamma_{d11}}{\mu_1})\sigma_1^2 \lambda_1^{*2}}}{2(1 - \frac{a_{11}^{(\phi)}}{\mu + a_{11}^{(\Omega)}} \frac{\gamma_{d11}}{\mu_1})}} \tag{32}$$

2.3. Numerical solution

A numerical solution using the Harmonic Polynomial Cell (HPC) method has been implemented. The HPC method is a field method initially described by Shao and Faltinsen (2014a,b) to solve the Laplace equation with boundary conditions for an unknown velocity potential. In the HPC method, the local expression of the velocity potential within a cell uses harmonic polynomials. Hence, the governing equation is satisfied naturally. The connectivity between different cells is built by overlapping the local expressions. A key feature of the HPC method is in using higher-order local expressions satisfying Laplace equation, which means that we can expect a better accuracy than for many other low order field and boundary integral formulations presently used. Moreover, the HPC method operates with a sparse coefficient matrix, so that many existing numerical matrix solvers can solve the associated problem efficiently.

The solution by the HPC method is based on representing the velocity potential as

$$\Phi = \sum_{m=0}^{M} \phi_m \dot{v}_m \tag{33}$$

where $v_0 = \eta_2$ and $U_0 = 1$ and ϕ_m satisfy the body boundary condition

$$\left.\frac{\partial \phi_m}{\partial y}\right|_{y=-l/2} = U_m(z) \tag{34}$$

together with homogenous Neumann conditions at $y = l/2$ for $m \geq 1$ and $\partial\phi_0 \partial y = 1$ at $y = l/2$, homogenous Neumann conditions at $z = -h$ and the combined free surface condition following from eq. 7 and eq.8. The 2D membrane is solved numerically by a modal representation, as for the analytical solution, where the deformation is given by eq. 5. Eq. 22 is used to find ν_j by first expressing the right hand side in terms in terms of generalized added mass coefficients a_{jm} defined as follows

$$\rho_w \int_{-h}^{0} \frac{\partial \Phi}{\partial t} U_j(z) dz = -\sum_{m=0}^{M} a_{jm} \ddot{\nu}_m, j = 1..M \tag{35}$$

$$a_{jm} = -\int_{-h}^{0} \phi_m U_j(z) dz \tag{36}$$

Simpson's integration method is used. The expressions are controlled by using that $a_{jm} = a_{mj}$ for j between 1 and M. The latter follows by using Green's second identity

$$\int_{S_F + S_B} \left[\phi_j \frac{\partial \phi_m}{\partial n} - \phi_m \frac{\partial \phi_j}{\partial n} \right] dS$$

together with boundary conditions on the mean the free surface S_F and on the mean wetted tank surface S_B and using that $\partial/\partial n$ means derivative along surface normal.

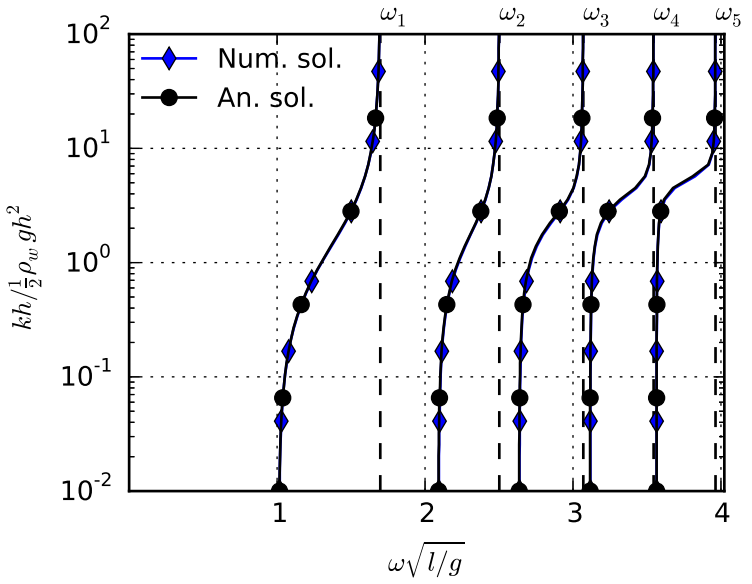

Figure 2: Non-dimensional eigenfrequencies of the coupled system eigenfrequencies $\omega_n^*\sqrt{l/g}$ for given stiffness $kh/\frac{1}{2}\rho_w gh^2$ for a rectangular tank with a rigid moving left wall. ω_n is the sloshing eigenfrequency for the rigid tank. Water depth (h)-to- l tank length ratio=0.5.

3. Case simulation results

To better get an understanding of how the system behaves, two main test cases have been run. For both cases, a 2D sloshing tank is used. The water depth-to-tank length ratio h/l is 0.5. Furthermore, wall thickness-to-tank length ratio is $d/l = 2.5 \cdot 10^{-3}$ and water density to solid wall density is $\rho_w/\rho_c = 1$. The fist case is with a rigid movable left wall with a spring attached, as described by Lu et al. (1997) and Chai et al. (1996). The second case is with a membrane left wall.

3.1. Case simulation results, movable wall

A special case of what we consider is that the wall moves as a rigid body, which corresponds to $U_m = 1$. This case have earlier been studied by Lu et al. (1997) and Chai et al. (1996). The relations in the coupled system is given by eq. 30 with the coefficients for this particular system given as $\mu = \rho_c dh$, $\lambda_k^2 = k/\mu$, where k is a spring stiffness and the coefficients $c^{rw} = \frac{\rho_w g h^2}{l}$, $a^{rw,(\Omega)} = \frac{\rho_w h}{3l}(l^2 + h^2)$ and $a^{rw,(\phi)}\gamma_d^{rw} = \rho_w \frac{2l^2}{(n\pi)^3}\tanh(k_n h)$, where rw stands for rigid wall.

The eigenfrequencies for the analytical solution has been estimated as a function of the spring stiffness k by considering when the determinant of the coupled system becomes zero. The non-dimensional eigenfrequencies $\omega_n^*\sqrt{l/g}$ of the system for different stiffness, for the case where the wall moves as a rigid body is plotted in figure 2. The analytical and the numerical solution based on the HPC method give the same eigenfrequencies. These eigenfrequencies also agree with the eigenfrequencies found by the method of Lu et al. (1997).The eigenfrequencies ω_n^* are dependent on the spring stiffness k. From figure 2 we see that $\omega_n^* \leq \omega_n$ as analytically shown by Schulkes (1990). When $k \to 0$, the dry eigenfrequency $\lambda_k \to 0$, but since the coupled fluid structure problem still have stiffness from the free surface stiffness term c^{rw}, the first eigenfrequency ω_1^* is finite.

3.2. Case simulation results, flexible wall

A test case with a flexible membrane wall with two different membrane wall lengths L ($L = h$ and $L = h$), and different tensions were then investigated.

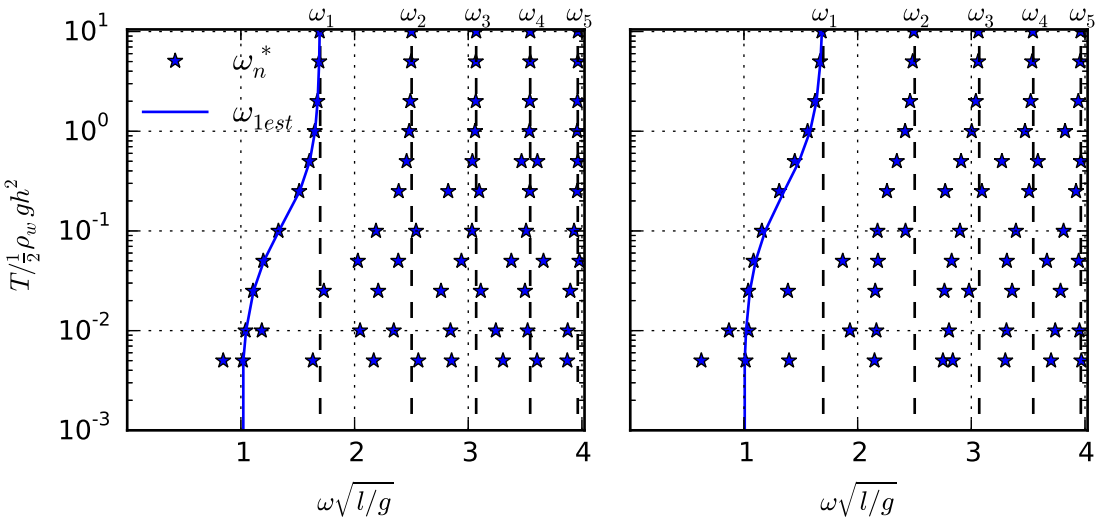

Figure 3: Non-dimensional eigenfrequencies of the coupled system eigenfrequencies $\omega_n^*\sqrt{l/g}$ for given tensions T/T_0 where $T_0 = \frac{1}{2}\rho_w g h^2$ for a rectangular tank with a membrane at the left wall. ω_n is the sloshing eigenfrequency for the rigid tank. Water depth (h)-to- l tank length ratio=0.5. Membrane length left: $L = h$. Right: $L = 2h$.

3.2.1. Eigenfrequencies of the coupled system

The eigenfrequencies for the analytical solution have been estimated as a function of the tension T by considering when the determinant of the coupled system becomes zero. Even though the hydrostatic pressure is not applied to the system, the hydrostatic pressure force equal to $F_s = \frac{1}{2}\rho_w g h^2$ is a real physical quantity to compare the amount of tension applied to the system too. We therefore define $T_0 = F_s = \frac{1}{2}\rho_w g h^2$ and use T/T_0 which is a ratio between the tension forces and the hydrostatic pressure forces. Converged results have been obtained by increasing numbers J of structural modes and numbers N of generalized free-surface coordinates. The non-dimensional eigenfrequencies $\omega_n^*\sqrt{l/g}$ of the system for different tensions $T/T_0 \in [5{\cdot}10^{-3}, 10]$, for 2D membrane lengths $h/L = 1$ and $h/L = 2$ are plotted in figure 3.

The eigenfrequencies of the system are highly dependent on both the tension and the 2D membrane length. If we consider a given value of T/T_0, then the eigenfrequency ω_n^* of the coupled system is smaller than the sloshing frequency ω_n of the rigid tank for any given n. When $T/T_0 \to \infty$, $\omega_n^* \to \omega_n$. If T/T_0 is small, and we consider a given ω_n, then there can be more than n eigenfrequencies of the coupled system that is lower than ω_n.

The first mode eigenfrequency of the system, from free surface mode $n = 1$, and structural mode $j = 1$ can be nicely estimated with ω_{1s}^{est}, as can be seen from figure 2. The line of ω_{2s}^{est} is not plotted in the figure, and that is because it did not fit with the system frequencies. The higher ω_n^* are not direct solutions of eq. 32 with other n, j combinations, which indicates that these frequencies depend on more than one set of (n, j) terms. This result was expected since the rigid tank sloshing frequencies are located so closely together that it is plausible that more than one will influence the coupled eigenfrequency ω_n^* for $\omega_n^* > \omega_1$. The figure shows that lower eigenfrequencies ω_n^* than ω_{1s}^{est} exist for the two lowest investigated tensions T/T_0.

If the eigenfrequencies of the flexible membrane in figure 3 are compared to the eigenfrequencies of the rigid moving wall case displayed in figure 2, we see that one eigenfrequency ω_n^* converges to $\omega_n^*\sqrt{l/g} \approx 1$, for both the rigid movable wall and for the flexible membrane case when respectively T and $kh \to 0$ for the studied case. However, it is not general that this eigenfrequency of the system is close to $\sqrt{g/l}$, when $T \to 0$. The similarity of the eigenfrequencies can be explained as follows: In eq. 13 we represent the deformation mode as a Fourier series. If the constant term α_{0m} gives a much

larger contribution to the pressure for the first mode than the remaining terms, the effect would be that solution of the case with the membrane wall will approach the solution of the rigid moving wall case, for frequencies lower than the first sloshing frequency. Higher eigenfrequencies ω_n^* does not show the same trend of being comparable.

For $T > 0.1T_0$ the eigenfrequencies appear to be converged within the frequency range for number of structural modes $J \geq 3$ for both the 2D membrane lengths. However, as the tension decreases more structural modes come into play. For the coupled analysis it was observed that as long as $J, N \geq 6$, the eigenfrequencies of the system did not change with increasing N, J for the given tension interval. This result would indicate that all the eigenfrequencies for the studied cases are within the first six eigenmodes.

3.2.2. Transfer function of free surface elevation of the coupled system

The analytical and numerical ratios ζ_a/η_{2a} (transfer function) between the wave amplitude at the right wall and the sway amplitude versus non-dimensional forcing frequency $\omega\sqrt{l/g}$ are plotted for the membrane length $L = h$ and $L = 2h$ in Figure 4 and 5, respectively. The non-dimensional tensions $T/T_0 = \frac{1}{4}, \frac{1}{2}, 1$ and 2 are examined. The analytical and numerical solutions agree very well, which support the correctness of both of them. Similar as for the eigenfrequencies plotted in figure 3 we see that the transfer functions are dependent on the tension in the system. The response goes to infinity at the eigenfrequencies of the system. If a rigid tank is considered, the system will have five eigenfrequencies in the considered frequency range. However, ω_2 and ω_4 correspond to even modes, and resonance oscillations at the right wall at these frequencies cannot be excited. For the tank with a flexible wall, we note resonant response at six eigenfrequencies for $T/T_0 = \frac{1}{4}$ and $T/T_0 = \frac{1}{2}$ and $L = 2h$. There are five eigenfrequencies for the other considered cases. When $L = h$, very narrow resonant response occurs close to ω_2 with $T/T_0 = \frac{1}{2}, 1$ and 2, and close to ω_4 with $T/T_0 = 1$ and 2. When $L = 2h$, very narrow resonant response occurs close to ω_2 with $T/T_0 = 1$ and 2. A large response is seen also between ω_3 and ω_4 for $T/T_0 = \frac{1}{2}$ for $L = h$, and between ω_3 and ω_5 for $T/T_0 = \frac{1}{2}$ and 1, for $L = 2h$. The response of the free surface rises to infinity at the eigenfrequencies, in agreement with linear potential flow theory of incompressible liquid.

More modes are needed in the analytical solution for the transfer function compared to the analysis of the eigenfrequencies to find the correct amplitude. In the calculation of the transfer function, 30 generalized free-surface coordinates β_n were used.

In the numerical solution, a square grid ($dx = dz$) with $N_x = 101$ nodes in the free surface were used. A convergence study has been run, and the results are converged. It was observed that for low tensions ($T < \frac{1}{4}T_0$) peaks in the transfer function showed up in the solution at the eigenfrequencies of the tank. These peaks vanished when the grid was refined. This cancellation effect can be seen by looking at eq. 30. When $\omega \to \omega_n$, the first and the last term in the eq. 30 will be much larger than the rest. Also, it can be assumed that the contributions from the given mode n, will be far greater than the other modes, reducing eq. 30 at the frequency limit $\omega \to \omega_n$ to:

$$\sum_m \gamma_{dnm}\overline{\nu}_m = \gamma_{2n}\overline{\eta}_2, \tag{37}$$

which means that at the sloshing eigenfrequency of the rigid tank, the resonance cancels and we get a frequency independent relation between the forced sway and the deformation. The practical implications of this are that for frequencies around the sloshing eigenfrequency of the rigid tank, a more refined grid is needed for this canceling effect to happen. If care is not shown in the numerical solution, numerical inaccuracies can cause unphysical resonances. It was the fact that we had the analytical solution that pointed out this numerical problem for the direct solution of the boundary value problem.

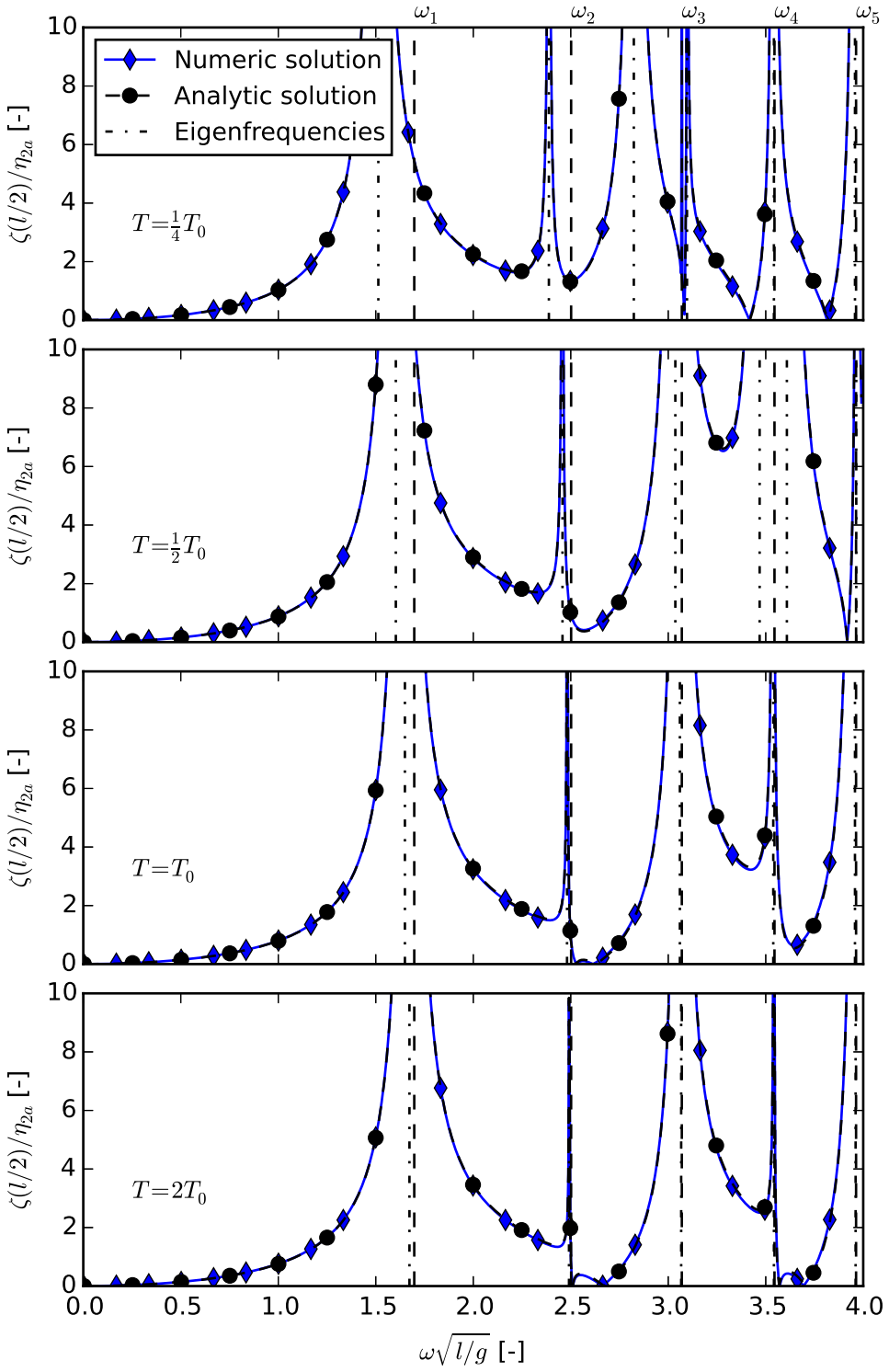

Figure 4: The analytical and numerical ratio $\frac{\zeta(l/2)}{\eta_{2a}}$ between the wave amplitude at the right wall ($\zeta(l/2)$)and the sway amplitude η_{2a} versus non-dimensional forcing frequency $\omega\sqrt{l/g}$ for forced sway oscillation of a rectangular tank with a membrane as the left wall. Water depth (h)-to- l tank length ratio=0.5. Membrane length $L = h$. Influence of non-dimensional membrane tension T/T_0 where $T_0 = \frac{1}{2}\rho_w g h^2$.

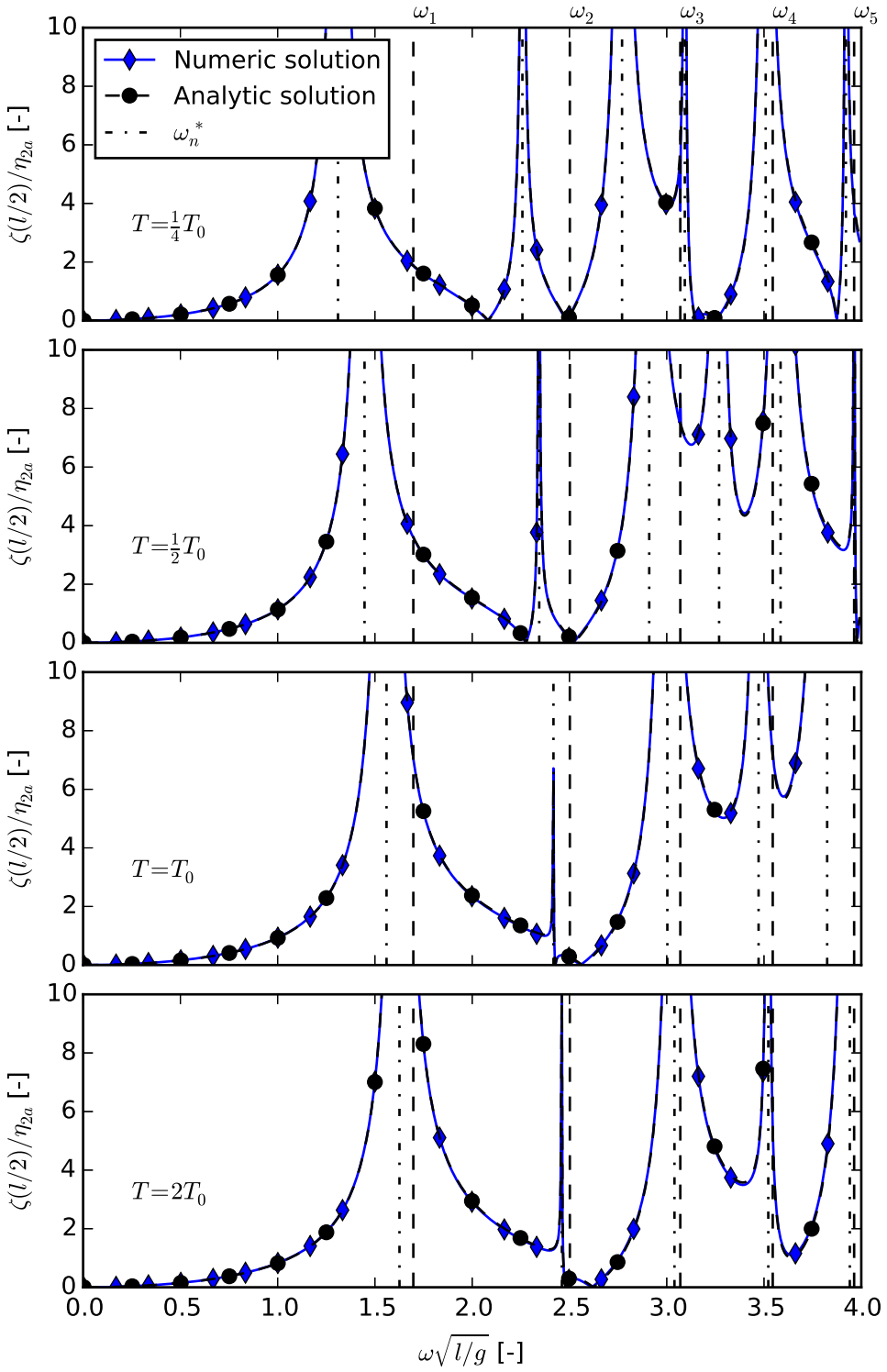

Figure 5: The analytical and numerical ratio $\frac{\zeta(l/2)}{\eta_{2a}}$ between the wave amplitude at the right wall ($\zeta(l/2)$)and the sway amplitude η_{2a} versus non-dimensional forcing frequency $\omega\sqrt{l/g}$ for forced sway oscillation of a rectangular tank with a membrane as the left wall. Water depth (h)-to- l tank length ratio=0.5. Membrane length $L = 2h$. Influence of non-dimensional membrane tension T/T_0 where $T_0 = \frac{1}{2}\rho_w g h^2$.

4. Conclusion and further work

A 2D rectangular sloshing tank with a flexible sidewall have been studied analytically and numerically, with a focus on coupling effects between sloshing and the flexible wall. Analytical and numerical solutions agree. The two cases are: one case with a rigid movable left wall with a spring attached. The second case is the tank with a flexible membrane left wall for different tensions and two different 2D membrane lengths ($L = h$ and $L = h$).

The eigenfrequencies of the system with a flexible membrane left wall, rely heavily on both tension and 2D membrane length. Number n eigenfrequency is lower than number n eigenfrequency of the rigid tank for finite tension. For low tensions, more than one eigenfrequency may exist between two neighbouring sloshing frequencies for the rigid tank. For large tensions, the eigenfrequencies of the system become the sloshing frequency of a rigid tank. For a given tension, one low eigenfrequency is found to involve interaction only between the lowest structural mode and sloshing mode. The other eigenfrequencies involve combinations of several structural and sloshing modes.

The analytical solution has provided important guidance for the numerical solution. If care is not shown in the numerical solution, numerical inaccuracies can cause unphysical resonances.

By comparing the analytical solution with the numerical solution, it has been shown that it is wrong to add a quasi-steady hydrostatic pressure change due to the time-dependent change in the mean free surface caused by the elastic wall deformations.

The response of the coupled system is infinite at the eigenfrequencies of the system, in reality, the amplitude must be finite. To find the actual response of the system, viscous damping and nonlinear free surface effects should be included; this is left for further work. In continuation of the presented work, we wish to use the gained knowledge and the validated numerical code to analyze the response of a semi-circular closed flexible fish cage in waves.

5. Acknowledgments

This work have been financed by the Research Council of Norway through the project "External Sea Loads and Internal Hydraulics of Closed Flexible Cages" (grant no. 216127). The work has been carried out at the Centre for Autonomous Marine Operations and Systems (AMOS), supported by the Research Council of Norway through the Centres of Excellence funding scheme, project number 223254 - AMOS. The Norwegian Research Council is acknowledged as the main sponsor of AMOS.

References

X. J. Chai, J. M. Genevaux, and J. P. Brancher. Fluid-solid interaction in a rectangular container. *European journal of mechanics. B, Fluids*, 15(6):865–883, 1996.

O. M. Faltinsen and A. N. Timokha. *Sloshing*. Cambridge University Press, 2009.

R. A. Ibrahim. *Liquid Sloshing Dynamics: Theory and Applications*. Cambridge: Cambridge UP, 2005.

M. H. Irvine. *Cable structures*. Cambridge, Mass.: The MIT Press, 1st edition, 1981.

P. Lader, D. W. Fredriksson, Z. Volent, J. DeCew, T. Rosten, and I. M. Strand. Drag Forces on, and Deformation of, Closed Flexible Bags. *Journal of Offshore Mechanics and Arctic Engineering*, 137 (August), 2015.

P. Lader, D. W. Fredriksson, Z. Volent, J. DeCew, T. Rosten, and I. M. Strand. Wave Response of Closed Flexible Bags. In *ASME 2016 35th International Conference on Ocean, Offshore and Arctic Engineering*, pages 1–10, 2016.

D. Lu, A. Takizawa, and S. Kondo. Overflow-induced vibration of a weir coupled with sloshing in a downstream tank. *Journal of Fluids and Structures*, 11(4):367 – 393, 1997.

S. Malenica, N. Vladimir, Y.M. Choi, I. Senjanovic, and S-H. . Kwon. Global hydroelastic model for liquid cargo ships. In *seventh International Conference on Hydroelasticity in Marine Technology, Split, Croatia*, 2015.

H. Rudi and F Solaas. Floating fish farms with bag pens. In *International Conference on Fish Farming Technology*, 1993.

R. M. S. M. Schulkes. Fluid oscillations in an open, flexible container. *Journal of Engineering Mathematics*, 24(3):237–259, 1990.

Y. Shao and O. M. Faltinsen. Fully-Nonlinear Wave-Current- Body Interaction Analysis by a Harmonic Polynomial Cell Method. *Journal of Offshore Mechanics and Arctic Engineering*, 136(August):8–13, 2014a.

Y. Shao and O. M. Faltinsen. A harmonic polynomial cell (HPC) method for 3D Laplace equation with application in marine hydrodynamics. *Journal of Computational Physics*, 274:312–332, 2014b.

I.M. Strand, A.J. Sørensen, and Z. Volent. Closed flexible fish cages: Modelling and control of deformations. In *Proceedings of 33rd International Conference on Ocean, Offshore and Arctic Engineering. June 8-13, 2014, San Francisco, USA*, 2014.

I.M. Strand, A.J. Sørensen, Z. Volent, and P. Lader. Experimental study of current forces and deformations on a half ellipsoidal closed flexible fish cage. *Journal of Fluids and Structures*, vol. 65, 2016.

Appendix A.

The different parts of the pressure contribution on the membrane with modes are calculated as:

$$\int_{-h}^{0}(\Omega_{dm}(-\frac{l}{2},z)-\overline{\Omega_{dm}})U_j(z)dz = \frac{a_{mj}^{(\Omega)}}{\rho_w} \tag{A.1}$$
$$= \Bigg[\alpha_{0m}\frac{L}{\pi jl}\left((\frac{2l^2}{3}+2\frac{L^2}{\pi^2j^2})\sin^2(\frac{\pi hj}{2L})-\frac{L}{\pi j}h\sin(\frac{\pi hj}{L})+\frac{h^2}{2}\right)$$
$$+\sum_{k=1}^{\infty}\alpha_{km}L\left(\frac{h}{k\pi}\right)^2\left(\frac{kjh((-1)^k\cos(\frac{j\pi h}{L})-1)}{\tanh(\pi kl/h)(L^2k^2-h^2j^2)}-\frac{2(-1)^k\sin^2(\frac{j\pi h}{2L})}{lj\pi}\right)\Bigg]$$

$$\frac{l}{2}\int_{-h}^{0}U_j(z)dz = \frac{\gamma_{2j}}{\rho_w} = \frac{lL}{j\pi}\sin^2(\frac{j\pi h}{2L}) \tag{A.2}$$

$$\int_{-h}^{0}\frac{\cosh(\pi n(z+h)/l)}{\kappa_n\cosh(\pi nh/l)}U_j(z)dz = \frac{a_{nj}^{(\phi)}}{\rho_w} \tag{A.3}$$
$$= \frac{l^2L(jl\cosh(\frac{\pi nh}{l})\cos(\frac{j\pi h}{L})-Ln\sinh(\frac{\pi nh}{l})\sin(\frac{j\pi h}{L})-jl)}{\pi^2n\sinh(\frac{\pi nh}{l})(L^2n^2+j^2l^2)}$$

$$\frac{g}{l}\int_{-h}^{0}U_m(z)dz\int_{-h}^{0}U_j(z)dz = \frac{c_{mj}}{\rho_w} = \frac{g}{l}\frac{4L^2}{mj\pi^2}\sin^2(\frac{j\pi h}{2L})\sin^2(\frac{m\pi h}{2L}) \tag{A.4}$$